



Published in final edited form as:

Ther Deliv. 2010 August ; 1(2): 289–305.

Overcoming the challenges in the effective delivery of chemotherapies to CNS solid tumors

Hemant Sarin

National Institute of Biomedical Imaging and Bioengineering, National Institutes of Health, Bethesda, Maryland, 20892, USA, Tel.: +1 301 648 6458

Hemant Sarin: hemantsarin74@gmail.com

Abstract

Locoregional therapies, such as surgery and intratumoral chemotherapy, do not effectively treat infiltrative primary CNS solid tumors and multifocal metastatic solid tumor disease of the CNS. It also remains a challenge to treat such CNS malignant solid tumor disease with systemic chemotherapies, although these lipid-soluble small-molecule drugs demonstrate potent cytotoxicity *in vitro*. Even in the setting of a 'normalized' tumor microenvironment, small-molecule drugs do not accumulate to effective concentrations in the vast majority of tumor cells, which is due to the fact that small-molecule drugs have short blood half-lives. It has been recently shown that drug-conjugated spherical lipid-insoluble nanoparticles within the 7–10 nm size range can deliver therapeutic concentrations of drug fraction directly into individual tumor cells following systemic administration, since these functionalized particles maintain peak blood concentrations for several hours and are smaller than the physiologic upper limit of pore size in the VEGF-derived blood capillaries of solid tumors, which is approximately 12 nm. In this article, the physiologic and ultrastructural basis of this novel translational approach for the treatment of CNS, as well as non-CNS, solid cancers is reviewed.

Challenges in the effective treatment of CNS solid tumors & recent progress

CNS solid tumors constitute a diverse group of metastatic brain and spinal cord tumors, which arise from cells of peripheral tumors that have seeded the CNS (e.g., lung, breast and renal), as well as primary brain and spinal cord tumors, which arise from supporting cells of the CNS (e.g., astrocytes, oligodendrocytes and germ cells) [1]. Single metastatic lesions to the CNS and lower histological grade primary CNS tumors such as hemangioblastomas are subsets of CNS solid tumors that can be effectively treated on symptomatic clinical presentation via surgical excision and stereotactic radiotherapy [2–4]. However, the incidence of single metastatic lesions to the CNS [5] is much lower than that of multifocal metastatic disease to the CNS [6,7] and, likewise, the incidence of lower histological grade primary CNS tumors is lower than that of higher grade primary CNS tumors [5,8]. Multifocal metastatic disease to the CNS presents as multiple well-circumscribed small solid tumor foci that are disseminated throughout the CNS and are difficult to treat effectively with locoregional therapies [9,10], whereas higher grade primary CNS tumors, such as

© 2010 Future Science Ltd

Financial & competing interests disclosure: The author has no other relevant affiliations or financial involvement with any organization or entity with a financial interest in or financial conflict with the subject matter or materials discussed in the manuscript apart from those disclosed.

No writing assistance was utilized in the production of this manuscript.

malignant gliomas and medulloblastomas, present as poorly demarcated solid tumor masses with infiltrative small tumor colonies in adjacent functionally intact CNS tissue [11] and, therefore, are difficult to treat effectively with locoregional therapies such as surgery, stereotactic radiotherapy and direct intratumoral chemotherapy, or with intracavitary chemotherapy in the postoperative resection cavity [10,12–17]. Furthermore, it remains a challenge to treat multifocal metastatic and primary infiltrative CNS tumor disease effectively with **small-molecule chemotherapy drugs** [18], even though these small lipid-soluble and cationic lipid-soluble drugs demonstrate potent cytotoxicity *in vitro* and can permeate the capillary walls of CNS solid tumor blood capillaries in most cases [19–27]. The high rates of multiple metastases to the CNS and localized reoccurrences of infiltrative primary CNS solid tumors following resection is attributable to the failure of small-molecule chemotherapy drugs to accumulate to cytotoxic concentrations in the individual tumor cells of small solid tumor foci [28,29].

Lipid-soluble and cationic lipid-soluble small-molecule chemotherapy drugs do not accumulate to cytotoxic concentrations in a significant proportion of solid tumor cells, irrespective of tumor location being within the CNS (CNS solid tumors)[30], or outside, in peripheral tissues (non-CNS solid tumors)[31,32]. In the 1980s, it was proposed that the primary reason for the ineffective accumulation of small molecule chemotherapy drugs into solid tumor cells is the elevated **interstitial fluid pressure (IFP)** of solid tumor interstitium, due to the ‘hyper-permeability’ of the VEGF-derived blood capillaries of solid tumors to macromolecules and the absence of the initial lymphatic capillaries and drainage in the tumor center [33–36]. Based on this reasoning, over the past several years low-to-moderate dose anti-VEGF therapies have been used to reduce the elevated solid tumor interstitial fluid pressure, in order to promote the better, more homogenous, distribution of adjuvantly administered small-molecule chemotherapy drugs within the solid tumor interstitium by causing the regression of solid tumor blood capillaries, as well as by inducing the conversion of solid tumor blood capillaries to a more normal, less permeable, phenotype (**vascular normalization**) [33,37–41]. It is notable, however, that the progression-free survival times of solid tumor patient populations treated with small-molecule chemotherapy drugs in combination with anti-VEGF therapies are only increased by a few months in most cases [42–45]. Based on such patient clinical outcome data, it can be inferred that, even with the normalization of the solid tumor blood capillary network and reduction of interstitial fluid pressure, small-molecule chemotherapy drugs do not accumulate to cytotoxic concentrations within a significant proportion of individual tumor cells in the solid tumor interstitium, which indicates that the elevated solid tumor IFP is not the primary reason for the ineffective accumulation of currently employed small-molecule systemic chemotherapies in the solid tumor interstitium and tumor cells. Other reasons have also been cited for the ineffectiveness of small-molecule drug accumulation in solid tumor cells, including limited drug bioavailability due to drug fraction being protein bound in systemic blood circulation [46] and the overexpression of p-glycoprotein (P-gp) and multidrug resistance-associated proteins (MRPs) in solid tumors, which are overexpressed on the cell membranes of the endothelial cells lining the blood capillary walls in the case of CNS solid tumors [47–49], and in the case of non-CNS solid tumors, on the cell membranes of the tumor cells themselves [50,51]. Although it is likely that these factors play some limited role in the ineffectiveness of small-molecule chemotherapy drugs, the overall ineffectiveness of small-molecule chemotherapies at treating solid tumors is attributable to the short blood half-life of small-molecule chemotherapy drugs [28,52], as these lipid-soluble and cationic lipid-soluble small-molecule drugs are rapidly metabolized, as well as efficiently filtered by the kidneys following bolus administration [53–56].

Recently, it has been shown that it is possible to deliver therapeutic concentrations of small-molecule drugs directly into solid tumor cells with small-molecule drug-conjugated lipid-

insoluble nanoparticles within the 7–10 nm size range [29,57]. This approach to the treatment of CNS solid tumors, as well as non-CNS solid tumors, takes advantage of the fact that:

- The blood capillary microvasculature of solid tumors is permeable to lipid-insoluble macromolecules as large as 12 nm in diameter, but not larger [28,58], as it is VEGF-derived fenestrated blood capillary microvasculature [59–61];
- Lipid-insoluble macromolecules 7 nm and larger in size, maintain peak blood concentrations for several hours [28], as macromolecules 7 nm and larger are not renally cleared [62].

In this review, the differences in the capillary wall morphology of normal brain and spinal cord parenchymal tissue and solid tumor tissue blood capillaries are highlighted and discussed in the context of the differences in the transcapillary routes for the passage of lipid-soluble and cationic lipid-soluble small-molecule drugs and lipid-insoluble small molecules and macromolecules, as these differences will need to be taken into consideration when designing lipid-insoluble macromolecular systemic therapies and **theranostics** within the 7–10 nm size range for CNS, as well as non-CNS, solid cancer treatment and monitoring of treatment response [28,58]. Furthermore, the issue of the functionalized nanoparticle exterior being cationic and resulting in cationic charge-mediated toxicity to the capillary wall is also discussed, as it will be important to ensure that the surface charge of functionalized lipid-insoluble macromolecules be maintained as neutral-to-anionic. In the future perspective, some of the foreseeable challenges to the successful translation of the proposed approach to the clinical setting are discussed [29].

Transcapillary routes for the passage of lipid-insoluble small molecules & macromolecules

The capillary walls of normal CNS and solid tumor tissue blood capillary microvasculatures are three-layered structures that consist of:

- The **endothelial glycocalyx layer** (EGL) on the luminal side;
- The basement membrane layer on the abluminal side;
- The endothelial cell lining layer in between the glycocalyx and the basement membrane (Figure 1A & B) [61,63–68].

The EGL is a polysaccharide-rich fibrous matrix of anionic proteoglycans and glycoproteins, and is a layer between 150 and 400 nm thick in most normal blood tissue capillary microvasculatures [69,70]. Although the exact thickness of this layer has not yet been determined in the cases of normal CNS tissue and CNS solid tumor tissue blood capillary microvasculatures, the glycocalyx is known to exist on the luminal surface of the endothelial cell lining in both these microvasculatures [63,64] and, in the case of solid tumor microvasculatures, it is attenuated in thickness (Figure 1A) [61]. The individual fibers of the glycocalyx matrix are thought to be hexagonally arranged and circumferentially spaced a maximum of 20 nm apart [71]. Therefore, this relatively narrow interspacing of the individual glycocalyx fibers is a physical barrier to the interaction of larger macromolecules and therapies with the endothelial cell lining layer, for example, of liposomes [72] and liposome-based therapies such as liposomal doxorubicin (diameter ~100 nm) (Figure 1A & B) [73]. By being rich in sialylated and sulphated glycoproteins and proteoglycans and by being anionic, the narrowly interspaced glycocalyx matrix fibers also constitute effective electrostatic barriers to the diffusion of blood globular proteins and immunoglobulins through the layer, which are anionic in systemic blood circulation [74,75].

The endothelial cell lining layer of normal brain and spinal cord parenchymal blood capillary walls is the site of the 'blood-brain barrier' (BBB), as it is a lining of juxtaposed endothelial cells that are nonfenestrated (Figure 1A) [66]. The capillary walls of normal brain and spinal cord parenchyma blood capillaries are permeable to small lipid-insoluble molecules (e.g., endogenous electrolytes and nonelectrolytes), since small aqueous pores exist in the zona occludens 'tight' junctional complexes that interconnect the endothelial cells that permit the transcapillary passage of small lipid-insoluble molecules with molecular weights of less than approximately 0.2 kDa, and diameters of less than approximately 1 nm [76,77], which constitutes the **physiologic upper limit of pore size** for the nonfenestrated blood capillaries that supply the normal brain and spinal cord parenchyma [68]. In the case of solid tumor tissue blood capillaries, the endothelial cell lining layer of the capillary walls is fenestrated [60,61], as the endothelial cells possess **diaphragmed fenestrae** with aqueous pores large enough to permit the transcapillary passage of lipid-insoluble macromolecules as large as 12 nm in diameter, but not larger (Figure 1B) [28,58]. Therefore, the physiologic upper limit of pore size for the VEGF-derived neo-angiogenic blood capillary microvasculature of CNS solid tumors, as well as non-CNS solid tumors located in peripheral tissues, is approximately 12 nm [28,58]. The observed tumor type and location-dependent differences in the regional permeabilities of solid tumor capillary beds to lipid-insoluble molecules and macromolecules are attributable to tumor type and location-dependent differences in the overall histological porous surface area available for transcapillary exchange [78–80], and not to differences in the upper limit of pore size in solid tumor blood capillary walls [28,58]. The widened and disrupted interendothelial cell junctions that have been noted on solid tumor blood capillary histopathology may also contribute to the permeability of solid tumor blood capillaries to lipid-insoluble molecules and macromolecules, but likely to a lesser extent than the aqueous pores of the diaphragmed fenestrae (Figure 1B) [61,68].

The abluminal basement membrane layer is composed of collagen type IV proteins and glycoproteins interlinked by proteoglycans with heparan sulphate glycosaminoglycan side chains, with the heparan sulphated proteoglycans being concentrated at the anionic sites of the basement membrane [81,82]. The basement membrane layer is between 60 and 100 nm thick in the capillary walls of both normal tissue and solid tumor tissue blood capillary microvasculatures (Figure 1A & B) [83–86]. The lattice of collagen fibrils of the basement membrane layer is not a significant restrictive barrier to the transcapillary extravasation of spherical macromolecules up to at least 12 nm in diameter (Figure 1B) [28,58,87]. In the case of the basement membrane of solid tumor tissue blood capillaries, it has been noted that there are occasional irregularities and focal defects [85,86,88]; however, these would not be expected to significantly alter the functionally restrictive properties of the layer due to their relative infrequency, which is why the basement membrane layers of normal brain and spinal cord parenchyma and solid tumor blood capillary microvasculatures are depicted as being similar in ultrastructure in Figure 1A & B.

Transcapillary routes for the passage of lipid-soluble & cationic lipid-soluble chemotherapy drugs

Since the 1960s, when systemic chemotherapies first began to be employed towards the clinical treatment of CNS solid tumors [89–91], small-molecule lipid-soluble and cationic lipid-soluble chemotherapies have formed the basis of chemotherapy regimens, which include traditional small-molecule chemotherapy drugs that target the cell cycle, such as DNA alkylators and antimetabolites [49,92], and newer small molecule drugs that target overexpressed tumor cell growth factor receptors and associated downstream cell-signaling pathways, including tyrosine kinase and proteasome inhibitors [23,93,94]. Most small-molecule chemotherapy drugs are lipid-soluble or cationic lipid-soluble molecules of

molecular weights less than 0.8 kDa with high octanol-water partition coefficients (K_{ow} ; LogP) and acid-dissociation constants (pK_a) [95]. Of these, the lipid-soluble and cationic lipid-soluble molecules of molecular weights less than approximately 0.4 kDa, such as lomustine (molecular weight 0.23 kDa; LogP 2.83 [95]) and temozolomide (molecular weight 0.19 kDa; LogP -0.66 [96]) can readily diffuse across the phospholipid bilayers of all cell membranes, including those of the endothelial cells that line all blood capillary walls [54–56,95,97], whereas those drugs with molecular weights greater than 0.4 kDa cannot diffuse as readily through phospholipid bilayers, which is the case for doxorubicin (molecular weight 0.54 kDa; LogP -0.10 [95]) (Figure 1A), vinblastine (molecular weight 0.91 kDa; LogP 1.68 [46]) and vincristine (molecular weight 0.92 kDa; LogP 2.14–2.80 [46,95]).

Cationic lipid-soluble drugs with molecular weights less than 0.2 kDa, such as temozolomide, being charged molecules, can also pass through the aqueous pores of the zona occludens interendothelial cell junctions to distribute into normal brain and spinal cord parenchyma (Figure 1A). Therefore, small drugs such as temozolomide can enter normal brain and spinal cord parenchyma interstitial spaces via both of these transcapillary routes, and can distribute more extensively into the normal CNS [92,98]. In contrast, doxorubicin, being a larger cationic lipid-soluble drug than temozolomide, and having a molecular weight greater than 0.4 kDa, is too large to readily diffuse through phospholipid bilayers and unable to diffuse through the aqueous pores of the zona occludens interendothelial cell junctions; therefore, doxorubicin does not distribute into the normal brain and spinal cord parenchyma interstitial spaces to any significant degree (Figure 1A) [25,95]. However, doxorubicin does readily distribute into the interstitial spaces of several normal non-CNS tissues, including skeletal and cardiac muscle tissues [99]. In the case of skeletal and cardiac muscle tissues, this is attributable to the capillary walls of the non-fenestrated blood capillaries of these tissues being lined by endothelial cells that are juxtaposed by macula occludens ‘loose’ junctional complexes, which permit the transcapillary passage of macromolecules as large as 5 nm in diameter [68,100]. These are the reasons for the clinically observed short- and long-term CNS and non-CNS tissue and organ toxicities associated with continuous, dose-intense and intra-arterial administration of lipid-soluble and cationic lipid-soluble small-molecule chemotherapy drugs [101–105], which nonselectively distribute into the interstitial spaces of both normal CNS and normal non-CNS tissues.

Lipid-soluble and cationic lipid-soluble chemotherapy drugs do not accumulate to cytotoxic concentrations in a significant proportion of tumor cells within the solid tumor interstitium. The primary reason for this is that lipid-soluble and cationic lipid-soluble drugs only remain at peak concentrations in systemic blood circulation for a few minutes following bolus administration, since these small-molecule drugs are rapidly metabolized as well as efficiently renally cleared.

Therefore, the concentration gradient favoring a net forward diffusion of these small molecule drugs across the capillary wall and into the solid tumor interstitial space is transient. Since the steep concentration gradient favoring transcapillary diffusion is only present for several minutes following the drug bolus, the net backward diffusion of drug molecules from the tumor interstitial space into the capillary lumen begins to occur as soon as the concentration gradient reverses, which is within a matter of minutes following the systemic bolus administration of drug (Figure 1A & B; bidirectional arrows). The forward concentration gradient, favoring small-molecule chemotherapy drug accumulation in the solid tumor interstitium, can be maintained by prolonging the blood half-life of the small-molecule drug chemotherapy, which can be increased either temporarily, via the coinfusion of a metabolically stable bradykinin B2 receptor agonist such as labradimil (Cereport[®] RMP-7) with the small drug [52,106,107], or for a more sustained duration, via continuous

small drug infusion [101–103]. In the latter case, in addition to small drug fraction accumulating to cytotoxic concentrations in the solid tumor interstitium, it also accumulates to toxic concentrations in the interstitial spaces of normal healthy tissues and results in patient morbidity and mortality [104–107].

Secondary reasons for small-molecule chemotherapy drugs not accumulating to cytotoxic concentrations in solid tumor cells include:

- A significant proportion of the administered drug fraction being protein bound in systemic blood circulation, which could be a secondary reason to explain why charged lipid-soluble drugs vinblastine (molecular weight 0.91 kDa; LogP 1.68 [46]) and vincristine (molecular weight 0.92 kDa, LogP 2.14–2.80 [46,95]) do not accumulate to therapeutic concentrations in CNS solid tumors [46];
- A significant proportion of administered drug fraction is effluxed back into systemic circulation by P-gp and MRPs overexpressed on the endothelial cells of CNS solid tumor blood capillaries [47], which could be a secondary reason why drugs such as temozolomide, doxorubicin, vinblastine and vincristine do not accumulate to therapeutic concentrations in CNS solid tumors [25,48,108];
- A significant proportion of the administered drug fraction that enters the tumor cells of non-CNS solid tumors is effluxed back into the tumor interstitium by P-gp and MRPs overexpressed on cell membranes of non-CNS solid tumor cells [50], which could be another secondary reason why drugs such as doxorubicin, vinblastine and vincristine do not accumulate to therapeutic concentrations in non-CNS solid tumor cells [51].

Therapeutic significance of the physiologic upper limit of pore size in solid tumor blood capillary walls

In order for systemic therapy to effectively treat solid cancers, it must remain at peak concentration in systemic blood circulation for a sufficiently long time to accumulate to cytotoxic concentrations within all possible individual tumor cells in the solid tumor interstitium, which is not the case for the small molecule chemotherapy drugs in current clinical use, which are less than 1–2 nm in diameter. Therefore, for systemic therapy to accumulate to cytotoxic concentrations in tumor cells, the therapy must be large enough that it is not renally cleared for several hours, which is the case for spherical lipid-insoluble macromolecules 7 nm and larger in diameter. Since only spherical lipid-insoluble macromolecules 7 nm and larger will accumulate to cytotoxic concentrations within individual solid tumor cells, and only those macromolecules smaller than the upper limit of pore size in the capillary wall of solid tumor blood capillaries will pass through the aqueous pores in the capillary wall into the solid tumor interstitium and enter the solid tumor cells, it is important to know what, precisely, is the physiologic upper limit of pore size in the capillary walls of the VEGF-derived fenestrated blood capillaries of solid tumors.

The physiologic upper limit of pore size in the VEGF-derived blood capillaries of CNS solid tumors was first reported as being approximately 12 nm in 2008, which was on the basis of a detailed series of dynamic contrast-enhanced MRI experiments to interrogate the upper limit of pore size in the blood capillaries of orthotopically grown RG-2 rodent gliomas, following the intravenous infusions of various-sized Gd–diethylene triamine pentaacetic acid (DTPA)-conjugated dendrimer nanoparticles ranging from 1.5 to 14 nm in diameter [28]. This finding, that the upper limit of pore size in the VEGF-derived blood capillaries of CNS solid tumors is approximately 12 nm, was then confirmed to be the case in non-CNS solid tumors as well, specifically in ectopically grown RG-2 gliomas [58]. Based on these findings, the physiologic upper limit of pore size in the capillary walls of the VEGF-derived fenestrated

blood capillaries that supply solid tumors is approximately 12 nm [28,58,68]. Even though the physiologic upper limit of pore size in the capillary walls of the overwhelming majority of blood capillaries in any given solid tumor is expected to be approximately 12 nm, there may be an occasional focal areas in solid tumor tissue where the three-layered ultrastructure of the solid tumor blood capillary wall is grossly disrupted, for example, in an area where there is microhemorrhagic transformation, in which case the upper limit of pore size would no longer be bounded at 12 nm; however, it is emphasized that such areas of the tumor constitute rarities. Transient modifications of the solid tumor blood capillary wall ultrastructure during localized pharmacological- [87,109,110], hyperthermia- [72,111] and high-dose radiotherapy-induced [112,113] include other exceptions, in which instances the upper limit of pore size of solid tumor blood capillary microvasculature is at least temporarily higher.

Optimal particle size range for macromolecular systemic therapies

In recent years, small-molecule lipid-soluble and cationic lipid-soluble chemotherapy drugs have delivered systemically via incorporation into polymers, for example, by the incorporation of drug into the aqueous interior of liposomes (liposomal doxorubicin, diameter ~100 nm; [114–117]), for the purposes of sustained small-molecule drug release in systemic blood circulation. These relatively large polymeric formulations of small molecule drugs are restricted from interacting with the capillary wall by the presence of the EGL and the relatively narrow circumferential spacing of the individual glycocalyx fibers (Figure 1A & B) [71]. The major drawback of this macromolecular systemic chemotherapy approach is that small molecule drugs are released within systemic circulation (Figure 1A & B) and then, upon release, rapidly metabolized and efficiently filtered by the kidneys, which is why released small drug fraction does not accumulate to high concentrations within individual tumor cells. The other drawback of this approach is, of course, the immunogenicity of pegylated liposomal drug carriers, which results in the accelerated clearance of these macromolecular therapies from blood circulation upon repeated administrations [118,119].

Based on our recent studies, in which we imaged the accumulation of various-sized lipid-insoluble spherical Gd–DTPA-conjugated dendrimer nanoparticles (Gd–dendrimers) within the solid tumor interstitium of RG-2 rodent malignant gliomas for several hours after bolus intravenous administration with high-resolution dynamic contrast-enhanced MRI, the optimal particle size range for the effective accumulation of systemic therapies within solid tumor cells is between 7 and 10 nm [28,29,57,58]. The lower bounds of the optimal particle size range is based on the observation that Gd–dendrimer nanoparticles smaller than 7 nm in diameter are relatively efficiently cleared from blood circulation via renal filtration and do not maintain peak concentrations over time in systemic blood circulation, which is why these smaller particles do not distribute homogeneously through the solid tumor interstitium for sufficiently long to accumulate to high concentrations within individual tumor cells (Figure 2A & B; Gd–generation 1 [G1] through Gd–generation 4 [G4] dendrimers) [28]. It is noteworthy that there is a relative lack of accumulation of the lower generation Gd–dendrimers, Gd–G1 through Gd–G4, in the tumor interstitium of the small RG-2 malignant gliomas, which are all less than 30 mm³ in total tumor volume (Figure 2B). This is primarily attributable to smaller RG-2 gliomas being less vascular than larger RG-2 gliomas [52]. Furthermore, since the overall porous surface area available for transcapillary exchange is less in smaller solid tumors than larger ones, there is significantly less small-molecule drug and MRI contrast agent (e.g., Gd–DTPA) accumulation in the solid tumor interstitium of smaller gliomas [28,52,58,120], as well as lower-grade gliomas [78,80,120]. Based on these observations, the primary reason that small-molecule chemotherapy drugs do not accumulate to cytotoxic concentrations in a significant proportion of solid tumor cells in the interstitial spaces of small and low-grade solid tumors is, in fact, short drug blood half-life [28,52].

There is the significant accumulation of Gd–G5 and Gd–G6 dendrimer nanoparticles over time in the tumor interstitium of larger RG-2 malignant gliomas, as well as the tumor interstitium of the smaller RG-2 malignant gliomas, which is attributable to the fact that Gd–G5 and Gd–G6 dendrimer nanoparticles maintain peak concentrations over several hours in systemic blood circulation (Figure 2A & B) [28,58]. The upper bounds of the optimal particle-size range of approximately 10 nm for effective transvascular drug delivery into the solid tumor interstitium has been established on the basis of a couple of observations. The first observation is that Gd–G8 dendrimer nanoparticles, being larger than 12 nm in diameter, are too large to extravasate across the pores in the capillary walls of the VEGF-derived blood capillaries of solid tumors, irrespective of tumor location or volume, which is why the physiologic upper limit of pore size in solid tumor blood capillaries is approximately 12 nm [28,58]. The second observation is that Gd–G7 dendrimer nanoparticles, being larger than 10 nm in diameter, are too large to extravasate across the pores in the capillary walls of the blood capillary microvasculature of some of the smaller RG-2 malignant gliomas, which is the basis for establishing the upper bounds of the optimal particle-size range as being approximately 10 nm (Figure 2B) [28,57].

Although the diffusion coefficients of the functionalized dendrimer nanoparticles in the tumor interstitial spaces of orthotopic and ectopic RG-2 gliomas have not been measured, the diffusion coefficients of endogenous globular proteins within this size range have been measured in the tumor interstitial spaces of intracerebral U87 malignant gliomas and subcutaneous MU89 melanomas, which are xenografted human malignant gliomas and melanomas in mice [121]. In the case of both intracerebral gliomas and subcutaneous melanomas, the interstitial diffusion coefficients of globular proteins within the 7–10-nm size range are not significantly different from the free diffusion coefficients of the respective proteins in phosphate buffered saline solution [121]. This is also likely to be the case for functionalized dendrimer nanoparticles in the 7–10-nm size range, based on our observations that functionalized G5 dendrimer nanoparticles (hydrodynamic diameter ~9 nm) distribute homogeneously within the solid tumor interstitium, which is apparent on dynamic contrast-enhanced MRI *in vivo* (Figure 2A & B) and accumulate to high concentrations within individual solid tumor cells, which is apparent on fluorescence microscopy *ex vivo* [28,29,58]. The findings, taken together, indicate that the ultrastructural arrangement of the collagen-rich extracellular matrix of the solid tumor interstitium is not a significant barrier to the diffusion of spherical macromolecules in the 7–10-nm size range and that spherical macromolecular systemic therapies in this size range can be delivered effectively into individual solid tumor cells of CNS solid tumors as well as non-CNS solid tumors [28,58]. These findings, however, cannot be extrapolated to the cases of immunoglobulin- and immunoglobulin fragment-based therapies, since these macromolecular therapies do not accumulate homogeneously within the solid tumor interstitium due to restricted diffusion through the solid tumor interstitium as a result of high-affinity binding to extracellular matrix antigens and nonspherical particle shapes [37,121–123].

Based on the determination that the optimal particle size for macromolecule-based systemic therapies is 7–10 nm, in 2009, the Gd–G5 doxorubicin dendrimer nanoparticle was developed as the prototype of a theranostic agent in the 7–10 nm size range for the concurrent imaging and treatment of solid tumors and tested for preliminary *in vivo* efficacy in the orthotopic RG-2 glioma model [29,57]. The doxorubicin is attached to approximately 8% of the terminal amines of the Gd–G5 dendrimer via acid-labile covalent linkages or hydrazone bonds [124], as the acid lability of hydrazone bonds facilitate the release of doxorubicin from the Gd–G5 doxorubicin dendrimer following dendrimer endocytosis into tumor cell endolysosomal compartments, after which the released free doxorubicin diffuses into the tumor cell nucleus and intercalates the DNA [29]. The preliminary study data of

CNS solid tumor regression studies in the RG-2 malignant glioma model showed significant short-term tumor regression in those animals receiving the Gd-G5 doxorubicin dendrimer [29,57]. However, this approach will need to be refined further before it is ready for clinical translation, as there is the introduction of cationic charge on the particle exterior following the attachment of doxorubicin to be considered.

Issue of charge-mediated toxicity to blood capillary walls by cationic macromolecular systemic therapies

Transient positive charge-induced toxicity to cellular membranes is the mechanism by which cationic vectors facilitate efficient cellular transfection *in vitro* [125] and is the proposed mechanism by which cell-penetrating peptides permeate cellular membranes *in vivo* [126–128]. The mechanism by which cationic macromolecules and therapies permeate the capillary walls of nonfenestrated blood capillaries that are otherwise not permeable to the neutral or anionic forms of the same macromolecule and therapy, appears to be as follows:

- The cationic charge-mediated toxicity to the anionic fibers of the EGL, which results in the exposure of the underlying endothelial cells;
- Cationic charge-mediated stimulation of endothelial cell phagoendocytic activity, which is minimal at baseline as these are nonreticulo endothelial cells;
- Transcapillary release of a small fraction of the phagoendocytosed cationic macromolecules into the basement membrane layer or pericapillary interstitial tissue [29,68].

It appears that by this type of mechanism cationized ferritin (diameter ~12 nm [129]) [130], cationized immunoglobulin G (hydrodynamic diameter ~11 nm [131]) [74], cationic drug (doxorubicin)-conjugated Gd-G5 dendrimer (diameter ~9 nm) [29,57], cationic dye (rhodamine B)-conjugated Gd-G5 dendrimer (diameter ~9 nm) [28,57] and cationic dye (rhodamine B)-conjugated Gd-G8 dendrimer (diameter ~13 nm) [28,57] ‘nonselectively’ permeate the capillary walls of normal brain and spinal cord parenchymal tissue blood capillaries and extravasate into normal healthy brain and spinal cord parenchyma, when the anionic forms of the respective macromolecules do not [28,57,58].

The EGL of the capillary walls of the VEGF-derived fenestrated blood capillaries supplying solid tumors is thinner [61] and, therefore, increased solid tumor blood capillary permeability is evident soon after capillary wall exposure to cationic charge. Tumor blood capillary permeability to cationic macromolecules less than 12 nm in diameter can increase significantly following toxicity to the glycocalyx fibers that flank the aqueous pores of the diaphragmed fenestrae, since macromolecules less than 12 nm in diameter can pass through the aqueous pores of the diaphragmed fenestrae of the capillary wall endothelial cells. This is the case for the following:

- Cationized IgG compared with the native IgG (hydrodynamic diameters ~11 nm) [132];
- Cationic drug (doxorubicin)-conjugated Gd-G5 dendrimer compared with the anionic Gd-G5 dendrimer (diameters ~9 nm) [28,29,57,58];
- Cationic dye (rhodamine B)-conjugated Gd-G5 dendrimer compared with the anionic Gd-G5 dendrimer (diameters ~9 nm) [28,29,57,58];
- Cationized albumin compared with native albumin (diameters ~7 nm [131])[132].

Since cationic macromolecules and therapies larger than 12 nm cannot extravasate to any appreciable extent across the aqueous pores of diaphragmed fenestrae, the mechanism by

which cationic macromolecules and therapies larger than 12 nm permeate the capillary walls of solid tumor blood capillaries is thought to be similar to that by which cationic macromolecules and therapies permeate the capillary walls of nonfenestrated blood capillaries. This is the case for cationic dye (rhodamine B)-conjugated Gd-G8 dendrimers (diameter ~13 nm), which do permeate the capillary walls of solid tumor blood capillaries, as compared with anionic Gd-G8 dendrimer (diameter ~13 nm), which do not permeate the capillary walls of solid tumor blood capillaries [28,29,57,58].

Larger cationic macromolecules, such as cationic liposomes (diameter ~90 nm) and cationic dye (rhodamine)-labeled liposomes (diameter range 100–600 nm), do not appear to permeate blood capillary walls of normal tissue blood capillaries for several hours after systemic infusion [72,133–137], which is in contrast to smaller cationic macromolecules that begin to permeate blood capillary walls within minutes of infusion [28,29,57]. In the case of blood capillaries that supply normal tissues and organs, the transcapillary permeation of cationic liposomes is relatively sparse even at 24–48 h after infusion [134,135], which is likely due to the existence of a full-thickness EGL layer in normal tissue blood capillary walls, in contrast to the thinner glycocalyx layer of solid tumor blood capillary walls [61]. In the case of solid tumor blood capillaries, however, there is evidence of cationic liposomal and cationic dye-labeled liposomal permeation into the pericapillary interstitial space in some cases [133,134] and, in other cases, permeation to what appears to be the level of the basement membrane layer [135], which is attributable to the restricted diffusion of these large cationic macromolecules through the collagen-rich fibrous lattices of the tumor interstitium and the capillary wall basement membrane layer, respectively [85,138]. The wide range of variability in the previously reported physiologic upper limits of pore size in the capillary walls of different solid tumor blood capillary microvasculatures is attributable to the fact that the physiologic upper limits of pore size in capillary walls of different solid tumor blood capillary microvasculatures were previously determined on the basis of intravital fluorescence microscopy of cationic dye (rhodamine)-labeled liposome transcapillary extravasation 24–48 h after cationic nanoparticle infusion, which is sufficient time for cationic charge-mediated toxicity to the tumor blood capillary walls and cationic liposome permeation of tumor blood capillary walls to some extent [136].

Future perspective

VEGF induces the formation of blood capillaries with capillary walls lined by fenestrated endothelial cells with diaphragmed fenestrae [60,139,140], with each diaphragmed fenestrae being perforated by several aqueous pores [141,142]. In the case of VEGF-derived blood capillaries of solid tumors [61], the aqueous pores of the endothelial cell is diaphragmed fenestrae, permitting the transcapillary passage of macromolecules up to 12 nm in diameter, but not larger, which is the therapeutically relevant upper limit of pore size for the effective transvascular delivery of systemic therapies into solid tumor cells (Figures 1B & 2A) [28,29,58].

The combination of solid tumor blood capillaries being ‘hyperpermeable’ to fluids and macromolecules, and the solid tumor center being devoid of the initial lymphatic capillaries and lymphatic drainage, results in the accumulation of blood plasma water and globular proteins over time within the solid tumor interstitium and increases the interstitial fluid pressure within the solid tumor interstitium [33,143]. This pathophysiology of the solid tumor interstitium was noted in the 1980s as being the basis for the ‘enhanced permeation and retention’ of systemically administered poly(styrene-comaleic acid)-neocarzinostatin (molecular weight 16 kDa) in non-CNS solid tumors [31,143,144], which are amphiphilic macromolecules that noncovalently bind to blood proteins such as albumin and then extravasate, protein bound, through capillary wall pores into the solid tumor interstitium

[145], after which the drug-bound macromolecule–protein complexes enter tumor cells via endocytosis [146,147]. Since then, other subsequent translational efforts have been geared towards the development of macromolecular systemic chemotherapies in the 20–130 nm size range, such as antibody-targeted dendrimer–drug conjugates [148] and polymeric drug carriers [73,149,150] or, alternatively, chemotherapies in the 4–5 nm size range (molecular weights ~40–50 kDa [28]), such as small-molecule drug-conjugated dendrimers [124,151–154]. The main drawback of macromolecular systemic therapies in the 20–130 nm size range is that these therapies remain intravascular and release attached, encapsulated or noncovalently bound small molecule drugs in systemic circulation, which are rapidly metabolized and renally cleared after release and do not accumulate to effective concentrations in solid tumor cells. By contrast, the main drawback of systemic therapies in the 4–5 nm size range is that these macromolecular therapies do not accumulate in the solid tumor interstitium for sufficiently long to achieve maximally effective concentrations in all possible tumor cells, as these therapies are still renally cleared (Figure 2A & B; Gd–G4 dendrimer).

Over the past decade much emphasis has been placed on vascular normalization of the fenestrated phenotype of VEGF-derived solid tumor blood capillaries to reduce the ‘hyper-permeability’ of the microvasculature in order to lower the elevated interstitial fluid pressure of the solid tumor interstitium and promote the more homogenous distribution of concurrently administered small-molecule chemotherapy drugs in the solid tumor interstitium, which has previously been proposed to be the primary reason that small-molecule chemotherapy drugs do not accumulate to cytotoxic concentrations in a significant proportion of solid tumor cells [33]. It is notable, however, that anti-VEGF therapies only marginally improve the effectiveness of concurrently administered small molecule chemotherapy drugs in the clinical setting, as evidenced by the fact that solid tumor progression only slows for a few months in most cases [42]. Anti-VEGF therapies, however, do effectively lower the elevated solid tumor interstitial fluid pressure [39], which supports the viewpoint that elevated interstitial fluid pressure is, in fact, not the underlying reason for the failure of small-molecule chemotherapy drugs to accumulate to cytotoxic concentrations within a significant proportion of solid tumor cells, but that it is the small particle size of current systemic chemotherapies, which needs to be within the 7–10 nm range for systemic therapies to distribute homogeneously through the solid tumor interstitium and accumulate to therapeutic concentrations within solid tumor cells, independent of tumor location being in the CNS, or outside, in peripheral tissues [28,29,57,58].

Our recent findings demonstrate that the optimal particle size range for effective transvascular drug delivery into solid tumor cells is between 7–10 nm, and that a particle size difference of even a few nanometers significantly affects systemic therapy delivery into solid tumor cells (Figure 2A & B) [28,29,57,58]. The proposed approach of employing drug-conjugated lipid-insoluble macromolecules in the 7–10 nm size range for the transcapillary delivery of covalently attached small molecule drugs into solid tumor cells is expected to be particularly effective in the treatment of solid tumors with multidrug-resistant tumor cell populations. This is due to the fact that a small-molecule drug covalently bound to a macromolecule (e.g., Gd–G5 doxorubicin dendrimer [29,57]) is not a substrate for P-gp and MRP small-drug efflux pumps, which are known to be overexpressed on cell membranes of endothelial cells that line CNS solid tumor blood capillary walls [47–49] and, in the case of non-CNS solid tumors, on the cell membranes of the tumor cells themselves [50,51]. However, it is foreseeable that, even with this approach, which indirectly addresses the problem of small-drug efflux at levels of both the endothelial cell membrane and the tumor cell membrane, drug-resistance issues at the intracellular and intranuclear levels will still need to be addressed. For example, in the case of DNA-repair enzyme O⁶-methylguanine methyltransferase-mediated drug resistance to DNA alkylating agents such as temozolomide

[49,155]. Furthermore, for the successful clinical translation of the proposed approach, it will be important to ensure that the chemotherapy-functionalized lipid-insoluble particles are within the optimal particle size range and also that the exterior of such particles remains neutral following drug attachment, in order to minimize cationic charge-based toxicity to the EGL layer of the capillary walls of normal tissue blood capillary microvasculatures [29,57]. It is envisioned that macromolecular systemic chemotherapies in the 7–10 nm size range will be effective treatments for non-CNS and CNS solid cancers.

Acknowledgments

The research was funded by the National Institute of Biomedical Imaging and Bioengineering, National Institutes of Health, Bethesda, Maryland 20892, USA.

Bibliography

Papers of special note have been highlighted as:

■ of interest

■ ■ of considerable interest

1. Louis DN, Ohgaki H, Wiestler OD, et al. The 2007 WHO classification of tumours of the central nervous system. *Acta Neuropathol.* 2007; 114(2):97. [PubMed: 17618441]
2. Patchell RA, Tibbs PA, Walsh JW, et al. A randomized trial of surgery in the treatment of single metastases to the brain. *N Engl J Med.* 1990; 322(8):494–500. [PubMed: 2405271]
3. Weil RJ, Lonsler RR, DeVroom HL, Wanebo JE, Oldfield EH. Surgical management of brainstem hemangioblastomas in patients with von Hippel-Lindau disease. *J Neurosurg.* 2003; 98(1 Suppl): 95–105. [PubMed: 12546357]
4. Moss JM, Choi CY, Adler JR Jr, Soltys SG, Gibbs IC, Chang SD. Stereotactic radiosurgical treatment of cranial and spinal hemangioblastomas. *Neurosurgery.* 2009; 65(1):79–85. [PubMed: 19574828]
5. Wohrer A, Waldhor T, Heinzl H, et al. The Austrian brain tumour registry: a cooperative way to establish a population-based brain tumour registry. *J Neurooncol.* 2009; 95(3):401–411. [PubMed: 19562257]
6. Barnholtz-Sloan JS, Sloan AE, Davis FG, Vignea FD, Lai P, Sawaya RE. Incidence proportions of brain metastases in patients diagnosed (1973 to 2001) in the Metropolitan Detroit Cancer Surveillance System. *J Clin Oncol.* 2004; 22(14):2865–2872. [PubMed: 15254054]
7. Eichler AF, Plotkin SR. Brain metastases. *Curr Treat Options Neurol.* 2008; 10(4):308–314. [PubMed: 18579017]
8. Brown M, Schrot R, Bauer K, LeTendre D. Incidence of first primary central nervous system tumors in California, 2001–2005. *J Neurooncol.* 2009; 94(2):263–273. [PubMed: 19340399]
9. Melisko ME, Glantz M, Rugo HS. New challenges and opportunities in the management of brain metastases in patients with ErbB2-positive metastatic breast cancer. *Nat Clin Pract Oncol.* 2009; 6(1):25. [PubMed: 18936791]
10. Ranjan T, Abrey LE. Current management of metastatic brain disease. *Neurotherapeutics.* 2009; 6(3):598. [PubMed: 19560748]
- 11 ■. Demuth T, Berens ME. Molecular mechanisms of glioma cell migration and invasion. *J Neurooncol.* 2004; 70(2):217–228. Provides insight into the molecular pathways involved in glioma cell migration, which could be potential future therapeutic targets. [PubMed: 15674479]
12. Laws ER, Parney IF, Huang W, et al. Survival following surgery and prognostic factors for recently diagnosed malignant glioma: data from the glioma outcomes project. *J Neurosurg.* 2003; 99(3):467–473. [PubMed: 12959431]
13. Bidros DS, Liu JK, Vogelbaum MA. Future of convection-enhanced delivery in the treatment of brain tumors. *Future Oncol.* 2010; 6(1):117–125. [PubMed: 20021213]

14. Hart, MG.; Grant, R.; Garside, R.; Rogers, G.; Somerville, M.; Stein, K. Cochrane Database of Systematic Reviews. John Wiley and Sons, Ltd; NY, USA: 2010. Chemotherapeutic wafers for high grade glioma.
15. Debinski W, Tatter SB. Convection-enhanced delivery for the treatment of brain tumors. *Expert Rev Neurother.* 2009; 9(10):1519–1527. [PubMed: 19831841]
16. Brem SS, Bierman PJ, Black P, et al. Central nervous system cancers: clinical practice guidelines in oncology. *J Natl Compr Canc Netw.* 2008; 6(5):456–504. [PubMed: 18492461]
- 17■. Anderson E, Grant R, Lewis SC, Whittle IR. Randomized Phase III controlled trials of therapy in malignant glioma: where are we after 40 years? *British J Neurosurg.* 2008; 22(3):339–349. A meta-analysis of malignant glioma patient outcome data from 44 clinical trials between 1966 and 2004, which draws attention to the fact that there has been relatively little improvement in patient outcomes over the years.
- 18■■. Muldoon LL, Soussain C, Jahnke K, et al. Chemotherapy delivery issues in central nervous system malignancy: a reality check. *J Clin Oncol.* 2007; 25(16):2295–2305. Highlights the historical challenge of effective drug delivery into the CNS across blood–brain, blood–tumor, and blood–cerebrospinal fluid barriers, and highlights the need for the development of innovative treatment and drug delivery approaches into CNS solid malignancies. [PubMed: 17538176]
19. Hildebrand J, Gorlia T, Kros JM, et al. Adjuvant dibromodulcitol and BCNU chemotherapy in anaplastic astrocytoma: results of a randomised European organisation for research and treatment of cancer Phase III study (EORTC study 26882). *Eur J Cancer.* 2008; 44(9):1210–1216. [PubMed: 18248979]
20. Grundy RG, Wilne SH, Robinson KJ, et al. Primary postoperative chemotherapy without radiotherapy for treatment of brain tumours other than ependymoma in children under 3 years: results of the first UKCCSG/SIOP CNS 9204 trial. *Eur J Cancer.* 2010; 46(1):120–133. [PubMed: 19818598]
21. Nicolaidis T, Tihan T, Horn B, Biegel J, Prados M, Banerjee A. High-dose chemotherapy and autologous stem cell rescue for atypical teratoid/rhabdoid tumor of the central nervous system. *J Neurooncol.* 2009; 98(1):117–123. [PubMed: 19936623]
22. Van Genugten JAB, Leffers P, Baumert BG, Tjon-A-Fat H, Twijnstra A. Effectiveness of temozolomide for primary glioblastoma multiforme in routine clinical practice. *J Neurooncol.* 2010; 96(2):249–257. [PubMed: 19582373]
23. De Witt Hamer PC. Small molecule kinase inhibitors in glioblastoma: a systematic review of clinical studies. *Neuro Oncol.* 2010; 12(3):304–316. [PubMed: 20167819]
24. Fangusaro J. Pediatric high-grade gliomas and diffuse intrinsic pontine gliomas. *J Child Neurol.* 2009; 24(11):1409–1417. [PubMed: 19638636]
25. Von Holst H, Knochenhauer E, Blomgren H, et al. Uptake of adriamycin in tumour and surrounding brain tissue in patients with malignant gliomas. *Acta Neurochir.* 1990; 104(1–2):13–16.
26. Stupp R, Hegi ME, Mason WP, et al. Effects of radiotherapy with concomitant and adjuvant temozolomide versus radiotherapy alone on survival in glioblastoma in a randomised Phase III study: 5-year analysis of the EORTC-NCIC trial. *Lancet Oncol.* 2009; 10(5):459. [PubMed: 19269895]
27. Levin VA, Landahl HD, Freeman Dove MA. The application of brain capillary permeability coefficient measurements to pathological conditions and the selection of agents which cross the blood brain barrier. *J Pharmacokinet Biopharm.* 1976; 4(6):499. [PubMed: 827606]
- 28■■. Sarin H, Kanevsky A, Wu H, et al. Effective transvascular delivery of nanoparticles across the blood–brain tumor barrier into malignant glioma cells. *J Transl Med.* 2008; 6(80) First study to report that the physiologic upper limit of pore size of the VEGF-derived blood capillaries of CNS solid tumors is approximately 12 nm, based on the findings of a large body of experimental data on presented and discussed in context of the importance of particle blood half-life for effective transcapillary drug delivery into individual solid tumor cells.
- 29■■. Sarin H. Recent progress towards development of effective systemic chemotherapy for the treatment of malignant brain tumors. *J Transl Med.* 2009; 7:77. Preliminary therapeutic efficacy of a prototypical drug-conjugated imageable dendrimer (Gd–G5 doxorubicin dendrimer) in the

- RG-2 rodent malignant glioma model *in vivo*, which is a macromolecular therapy in the 7–10 nm size range. [PubMed: 19723323]
30. Vick NA, Khandekar JD, Bigner DD. Chemotherapy of brain tumors The 'blood–brain barrier' is not a factor. *Arch Neurol.* 1977; 34(9):523. [PubMed: 889492]
 31. Maeda H, Matsumoto T, Konno T, Iwai K, Ueda M. Tailor-making of protein drugs by polymer conjugation for tumor targeting: a brief review on SMANCS. *J Protein Chem.* 1984; 3(2):181–193.
 32. Tredan O, Galmarini CM, Patel K, Tannock IF. Drug resistance and the solid tumor microenvironment. *J Natl Cancer Inst.* 2007; 99(19):1441–1454. [PubMed: 17895480]
 33. Jain RK. Transport of molecules across tumor vasculature. *Cancer Metastasis Rev.* 1987; 6:559–593. Initial discussions on the existence of elevated hydrostatic and oncotic pressures of the solid tumor interstitium and relevance to the ineffectiveness of small molecule chemotherapy drug accumulation in solid tumor cells. [PubMed: 3327633]
 34. Baxter LT, Jain RK. Transport of fluid and macromolecules in tumors I Role of interstitial pressure and convection. *Microvasc Res.* 1989; 37(1):77. [PubMed: 2646512]
 35. Casley-Smith JR. The role of the endothelial intercellular junctions in the functioning of the initial lymphatics. *Angiologica.* 1972; 9(2):106. [PubMed: 4564848]
 36. Leu AJ, Berk DA, Lymboussaki A, Alitalo K, Jain RK. Absence of functional lymphatics within a murine sarcoma: a molecular and functional evaluation. *Cancer Res.* 2000; 60(16):4324–4327. [PubMed: 10969769]
 37. Jain RK, Baxter LT. Mechanisms of heterogeneous distribution of monoclonal antibodies and other macromolecules in tumors: significance of elevated interstitial pressure. *Cancer Res.* 1988; 48(24 Part 1):7022–7032. [PubMed: 3191477]
 38. Tong RT, Boucher Y, Kozin SV, Winkler F, Hicklin DJ, Jain RK. Vascular normalization by vascular endothelial growth factor receptor 2 blockade induces a pressure gradient across the vasculature and improves drug penetration in tumors. *Cancer Res.* 2004; 64(11):3731–3736. [PubMed: 15172975]
 39. Jain RK, Tong RT, Munn LL. Effect of vascular normalization by antiangiogenic therapy on interstitial hypertension, peritumor edema, and lymphatic metastasis: insights from a mathematical model. *Cancer Res.* 2007; 67(6):2729–2735. [PubMed: 17363594]
 40. Jain RK. Normalization of tumor vasculature: an emerging concept in antiangiogenic therapy. *Science.* 2005; 307(5706):58–62. [PubMed: 15637262]
 41. Yuan F, Chen Y, Dellian M, Safabakhsh N, Ferrara N, Jain RK. Time-dependent vascular regression and permeability changes in established human tumor xenografts induced by an antivascular endothelial growth factor/vascular permeability factor antibody. *Proc Natl Acad Sci USA.* 1996; 93(25):14765–14770. [PubMed: 8962129]
 42. Jain RK, Duda DG, Clark JW, Loeffler JS. Lessons from Phase III clinical trials on anti-VEGF therapy for cancer. *Nat Clin Prac Oncol.* 2006; 3(1):24–40. Patient outcome data from several anti-VEGF therapy clinical trials is collated and discussed.
 43. Cohen MH, Shen YL, Keegan P, Pazdur R. FDA drug approval summary: bevacizumab (Avastin[®]) as treatment of recurrent glioblastoma multiforme. *Oncologist.* 2009; 14(11):1131–1138. [PubMed: 19897538]
 44. Friedman HS, Prados MD, Wen PY, et al. Bevacizumab alone and in combination with irinotecan in recurrent glioblastoma. *J Clin Oncol.* 2009; 27(28):4733–4740. [PubMed: 19720927]
 45. Verhoeff JJC, Lavini C, van Linde ME, et al. Bevacizumab and dose-intense temozolomide in recurrent high-grade glioma. *Ann Oncol.* 2010 Epub ahead of print. 10.1093/annonc/mdp591
 46. Greig NH, Soncrant TT, Shetty HU, Momma S, Smith QR, Rapoport SI. Brain uptake and anticancer activities of vincristine and vinblastine are restricted by their low cerebrovascular permeability and binding to plasma constituents in rat. *Cancer Chemother Pharmacol.* 1990; 26(4):263. [PubMed: 2369790]
 47. Toth K, Vaughan M, Peress N, Slocum H, Rustum Y. MDR1 P-glycoprotein is expressed by endothelial cells of newly formed capillaries in human gliomas but is not expressed in the neovasculature of other primary tumors. *Am J Pathol.* 1996; 149(3):853–858. [PubMed: 8780389]

48. Schaich M, Kestel L, Pfirrmann M, et al. A MDR1 (ABCB1) gene single nucleotide polymorphism predicts outcome of temozolomide treatment in glioblastoma patients. *Ann Oncol.* 2009; 20(1): 175–181. [PubMed: 18687982]
49. Sarkaria JN, Kitange GJ, James CD, et al. Mechanisms of chemoresistance to alkylating agents in malignant glioma. *Clin Cancer Res.* 2008; 14(10):2900–2908. [PubMed: 18483356]
50. Toth K, Vaughan MM, Schwartz G, et al. Expression of the MRP and MDR1 multidrug resistance gene products in 160 untreated human carcinomas studied by immuno-histochemical methods in formalin-paraffin sections. *Int J Surg Pathol.* 1998; 6(3):145–154.
51. Szakacs G, Annereau JP, Lababidi S, et al. Predicting drug sensitivity and resistance: profiling ABC transporter genes in cancer cells. *Cancer Cell.* 2004; 6(2):129–137. [PubMed: 15324696]
52. Sarin H, Kanevsky AS, Fung SH, et al. Metabolically stable bradykinin B2 receptor agonists enhance transvascular drug delivery into malignant brain tumors by increasing drug half-life. *J Transl Med.* 2009; 7:33. Evidence in support of drug blood half-life being the driving force for drug fraction accumulation to therapeutic concentrations in the solid tumor interstitium is presented. [PubMed: 19439100]
53. Hurria A, Lichtman SM. Clinical pharmacology of cancer therapies in older adults. *Br J Cancer.* 2008; 98(3):517–522. [PubMed: 18256586]
54. Jen JF, Cutler DL, Pai SM, et al. Population pharmacokinetics of temozolomide in cancer patients. *Pharm Res.* 2000; 17(10):1284–1289. [PubMed: 11145236]
55. Levin VA, Kabra PA, Freeman-Dove MA. Relationship of 1,3-bis(2-chloroethyl)-1-nitrosourea (BCNU) and 1-(2-chloroethyl)-3-cyclohexyl-1-nitrosourea (CCNU) pharmacokinetics of uptake, distribution, and tissue/plasma partitioning in rat organs and intracerebral tumors. *Cancer Chemother Pharmacol.* 1978; 1(4):233. [PubMed: 750110]
56. Levin VA, Kabra P. Effectiveness of the nitrosoureas as a function of their lipid solubility in the chemotherapy of experimental rat brain tumors. *Cancer Chemother Rep.* 1974; 58(6):787. [PubMed: 4447922]
57. Sarin, H. Effective transvascular delivery of chemotherapy into cancer cells with imageable nanoparticles in the 7–10 nanometer size range. In: Slevin, M., editor. *Current Advances in the Medical Application of Nanotechnology.* eBentham Books; 2010. In Press
58. Sarin H, Kanevsky A, Wu H, et al. Physiologic upper limit of pore size in the blood-tumor barrier of malignant solid tumors. *J Transl Med.* 2009; 7(51) First study to report that the physiologic upper limit of pore size in the VEGF-derived blood capillaries of both CNS solid tumors and non-CNS peripheral solid tumors is approximately 12 nm, as an extension of previous findings on the upper limit of pore size of CNS solid tumors. 10.1186/1479-5876-7-51
59. Folkman J, Klagsbrun M. Angiogenic factors. *Science.* 1987; 235(4787):442–447. Important review article as follow-up to Folkman's initial observations that VEGF drives the process of solid tumor neo-angiogenic blood capillary microvasculature, which is important for solid tumor growth beyond 1–2 mm³. [PubMed: 2432664]
60. Roberts WG, Palade GE. Neovasculature induced by vascular endothelial growth factor is fenestrated. *Cancer Res.* 1997; 57(4):765–772. Important study demonstrating that VEGF induces the formation of diaphragmed fenestrae in the endothelial cells of nonfenestrated blood capillaries such as those of skeletal muscle. [PubMed: 9044858]
61. Roberts WG, Delaat J, Nagane M, Huang S, Cavenee WK, Palade GE. Host microvasculature influence on tumor vascular morphology and endothelial gene expression. *Am J Pathol.* 1998; 153(4):1239–1248. Detailed morphometric data on the frequency of endothelial cell fenestration in the blood capillaries of intracranial solid tumors and subcutaneous solid tumors is presented. [PubMed: 9777955]
62. Bayliss LE, Kerridge PMT, Russell DS. The excretion of protein by the mammalian kidney. *J Physiol.* 1933; 77(4):386–398. [PubMed: 16994396]
63. Vorbrod AW. Ultracytochemical characterization of anionic sites in the wall of brain capillaries. *J Neurocytol.* 1989; 18(3):359–368. [PubMed: 2746307]
64. Schmidley JW, Wissig SL. Anionic sites on the luminal surface of fenestrated and continuous capillaries of the CNS. *Brain Res.* 1986; 363(2):265–271. [PubMed: 3942898]

65. Brightman MW. Morphology of blood-brain interfaces. *Exp Eye Res.* 1977; 25(Suppl):1–25. [PubMed: 73470]
66. Brightman MW, Reese TS. Junctions between intimately apposed cell membranes in the vertebrate brain. *J Cell Biol.* 1969; 40(3):648–677. [PubMed: 5765759]
67. Vick NA, Bigner DD. Microvascular abnormalities in virally-induced canine brain tumors Structural bases for altered blood–brain barrier function. *J Neurol Sci.* 1972; 17:29–39. [PubMed: 4341504]
68. Sarin H. Physiologic upper limits of pore size of different blood capillary types and another perspective on the dual pore theory of microvascular permeability. *J Angiogenesis Res.* 2010 In Press.
69. Pries AR, Secomb TW, Gaehtgens P. The endothelial surface layer. *Pflugers Arch.* 2000; 440(5): 653–666. [PubMed: 11007304]
70. Vink H, Duling BR. Identification of distinct luminal domains for macromolecules, erythrocytes, and leukocytes within mammalian capillaries. *Circ Res.* 1996; 79(3):581–589. [PubMed: 8781491]
71. Squire JM, Chew M, Nneji G, Neal C, Barry J, Michel C. Quasi-periodic substructure in the microvessel endothelial glycocalyx: a possible explanation for molecular filtering? *J Struct Biol.* 2001; 136(3):239–255. Arrangement and spacing of the fibers of endothelial glycocalyx layer is modeled on the basis of high-resolution atomic force microscopic visualization of the layer. [PubMed: 12051903]
72. Kong G, Braun RD, Dewhirst MW. Hyperthermia enables tumor-specific nanoparticle delivery: effect of particle size. *Cancer Res.* 2000; 60(16):4440–4445. [PubMed: 10969790]
73. Gabizon A, Chisin R, Amselem S, et al. Pharmacokinetic and imaging studies in patients receiving a formulation of liposome-associated adriamycin. *Br J Cancer.* 1991; 64(6):1125–1132. [PubMed: 1764376]
74. Triguero D, Buciak JB, Yang J, Pardridge WM. Blood–brain barrier transport of cationized immunoglobulin G: enhanced delivery compared with native protein. *Proc Natl Acad Sci USA.* 1989; 86(12):4761–4765. [PubMed: 2734318]
75. Weinbaum S, Zhang X, Han Y, Vink H, Cowin SC. Mechanotransduction and flow across the endothelial glycocalyx. *Proc Natl Acad Sci USA.* 2003; 100:7988–7995. Comprehensive review on the structure and biology of the endothelial glycocalyx layer of blood capillary walls. [PubMed: 12810946]
76. Fenstermacher JD, Johnson JA. Filtration and reflection coefficients of the rabbit blood–brain barrier. *Am J Physiol.* 1966; 211(2):341–346. [PubMed: 5921096]
77. Sorensen SC. The permeability to small ions of tight junctions between cerebral endothelial cells. *Brain Res.* 1974; 70(1):174–178. [PubMed: 4207049]
78. Jain R, Ellika SK, Scarpace L, et al. Quantitative estimation of permeability surface-area product in astroglial brain tumors using perfusion CT and correlation with histopathologic grade. *Am J Neuroradiol.* 2008; 29(4):694–700. [PubMed: 18202239]
79. Ludemann L, Grieger W, Wurm R, Wust P, Zimmer C. Quantitative measurement of leakage volume and permeability in gliomas, meningiomas and brain metastases with dynamic contrast-enhanced MRI. *Magn Reson Imaging.* 2005; 23(8):833. [PubMed: 16275421]
80. Provenzale JM, Wang GR, Brenner T, Petrella JR, Sorensen AG. Comparison of permeability in high-grade and low-grade brain tumors using dynamic susceptibility contrast MR imaging. *Am J Roentgenol.* 2002; 178(3):711. [PubMed: 11856703]
81. Leblond CP, Inoue S. Structure, composition, and assembly of basement membrane. *Am J Anat.* 1989; 185(4):367–390. [PubMed: 2675590]
82. Charonis AS, Wissig SL. Anionic sites in basement membranes Differences in their electrostatic properties in continuous and fenestrated capillaries. *Microvasc Res.* 1983; 25(3):265–285. [PubMed: 6855630]
83. Terayama N, Terada T, Nakanuma Y. An immunohistochemical study of tumour vessels in metastatic liver cancers and the surrounding liver tissue. *Histopathology.* 1996; 29(1):37–43. [PubMed: 8818692]

84. Carlson EC, Audette JL, Veitenheimer NJ, Risan JA, Laternus DI, Epstein PN. Ultrastructural morphometry of capillary basement membrane thickness in normal and transgenic diabetic mice. *Anat Rec A Discov Mol Cell Evol Biol.* 2003; 271A(2):332–341. [PubMed: 12629676]
85. Baluk P, Morikawa S, Haskell A, Mancuso M, McDonald DM. Abnormalities of basement membrane on blood vessels and endothelial sprouts in tumors. *Am J Pathol.* 2003; 163(5):1801–1815. [PubMed: 14578181]
86. Ludatscher RM, Gellei B, Barzilai D. Ultrastructural observations on the capillaries of human thyroid tumours. *J Pathol.* 1979; 128(2):57–62. [PubMed: 469654]
87. Muldoon LL, Pagel MA, Kroll RA, Roman-Goldstein S, Jones RS, Neuwelt EA. A physiological barrier distal to the anatomic blood-brain barrier in a model of transvascular delivery. *Am J Neuroradiol.* 1999; 20(2):217–222. [PubMed: 10094341]
88. Shibata S. Ultrastructure of capillary walls in human brain tumors. *Acta Neuropathol.* 1989; 78(6):561–571. [PubMed: 2554636]
89. Wilson CB, Gutin P, Boldrey EB. Single agent chemotherapy of brain tumors A five year review. *Arch Neurol.* 1976; 33(1):739–744. [PubMed: 185991]
90. Young CW, Burchenal JH. Cancer chemotherapy. *Annu Rev Pharmacol.* 1971; 11:369–386. [PubMed: 4948842]
91. Fewer D, Wilson CB, Boldrey EB, Enot KJ, Powell MR. The chemotherapy of brain tumors Clinical experience with carmustine (BCNU) and vincristine. *JAMA.* 1972; 222(5):549–552. [PubMed: 4343318]
92. Tentori L, Graziani G. Recent approaches to improve the anti-tumor efficacy of temozolomide. *Curr Med Chem.* 2009; 16(2):245–257. [PubMed: 19149575]
93. Knudsen BS, Vande Woude G. Showering c-MET-dependent cancers with drugs. *Curr Opin Genet Dev.* 2008; 18(1):87–96. Pros and cons of solid cancer treatment with small molecule inhibitors of the c-MET tyrosine kinase pathway are discussed. [PubMed: 18406132]
94. Schor NF. Pharmacotherapy for adults with tumors of the central nervous system. *Pharmacol Ther.* 2009; 121:253–264. [PubMed: 19091301]
95. Levin VA. Relationship of octanol/water partition coefficient and molecular weight to rat brain capillary permeability. *J Med Chem.* 1980; 23(6):682–684. [PubMed: 7392035]
96. Panassaya S, Guocheng W, Barbara RC, Weidong W, Yongfeng W. Skin delivery potency and anti-tumor activities of temozolomide ester prodrugs. *Cancer Lett.* 2006; 244(1):42–52. [PubMed: 16412562]
97. Pappenheimer JR. Passage of molecules through capillary walls. *Physiol Rev.* 1953; 33(3):387–423. Initial experimental and theoretical work that led to the formulation of the classic pore theory of microvascular permeability is presented. [PubMed: 13088295]
98. Newlands ES, Stevens MF, Wedge SR, Wheelhouse RT, Brock C. Temozolomide: a review of its discovery, chemical properties, preclinical development and clinical trials. *Cancer Treat Rev.* 1997; 23(1):35–61. [PubMed: 9189180]
99. Speth PAJ, Van Hoesel QGCM, Haanen C. Clinical pharmacokinetics of doxorubicin. *Clin Pharmacokinet.* 1988; 15(1):15–31. [PubMed: 3042244]
100. Karnovsky MJ. The ultrastructural basis of capillary permeability studied with peroxidase as a tracer. *J Cell Biol.* 1967; 35(1):213–236. [PubMed: 6061717]
101. Gill P, Litzow M, Buckner J, et al. High-dose chemotherapy with autologous stem cell transplantation in adults with recurrent embryonal tumors of the central nervous system. *Cancer.* 2008; 112(8):1805–1811. [PubMed: 18300237]
102. Dunkel IJ, Finlay JL. High-dose chemotherapy with autologous stem cell rescue for brain tumors. *Crit Rev Oncol Hematol.* 2002; 41(2):197–204. [PubMed: 11856595]
103. Dunkel IJ, Gardner SL, Garvin JH Jr, Goldman S, Shibata S. High-dose carboplatin, thiotepa, and etoposide with autologous stem cell rescue for patients with previously irradiated recurrent medulloblastoma. *J Clin Oncol.* 2010; 12(3):297–303.
104. Clarke JL, Iwamoto FM, Sul J, et al. Randomized Phase II trial of chemoradiotherapy followed by either dose-dense or metronomic temozolomide for newly diagnosed glioblastoma. *J Clin Oncol.* 2009; 27(23):3861–3867. [PubMed: 19506159]

105. Newton HB. Intra-arterial chemotherapy of primary brain tumors. *Curr Treat Options Oncol.* 2005; 6(6):519–530. [PubMed: 16242056]
106. Warren K, Gervais A, Aikin A, Egorin M, Balis FM. Pharmacokinetics of carboplatin administered with lobradimil to pediatric patients with brain tumors. *Cancer Chemother Pharmacol.* 2004; 54(3):206–212. [PubMed: 15156345]
107. Thomas HD, Lind MJ, Ford J, Bleehen N, Calvert AH, Boddy AV. Pharmacokinetics of carboplatin administered in combination with the bradykinin agonist Cereport (RMP-7) for the treatment of brain tumours. *Cancer Chemother Pharmacol.* 2000; 45(4):284. [PubMed: 10755316]
108. Decleves X, Amiel A, Delattre JY, Scherrmann JM. Role of ABC transporters in the chemoresistance of human gliomas. *Curr Cancer Drug Targets.* 2006; 6(5):433. [PubMed: 16918310]
109. Moore A, Marecos E, Bogdanov A, Weissleder R. Tumoral distribution of long-circulating dextran-coated iron oxide nanoparticles in a rodent model. *Radiology.* 2000; 214:568–574. [PubMed: 10671613]
110. Rapoport SI. Osmotic opening of the blood–brain barrier: principles, mechanism, and therapeutic applications. *Cell Mol Neurobiol.* 2000; 20(2):217. [PubMed: 10696511]
111. Kong G, Braun RD, Dewhirst MW. Characterization of the effect of hyperthermia on nanoparticle extravasation from tumor vasculature. *Cancer Res.* 2001; 61(7):3027–3032. [PubMed: 11306483]
112. Kobayashi H, Reijnders K, English S, et al. Application of a macromolecular contrast agent for detection of alterations of tumor vessel permeability induced by radiation. *Clin Cancer Res.* 2004; 10(22):7712–7720. [PubMed: 15570005]
113. Yordanov AT, Kobayashi H, English SJ, et al. Gadolinium-labeled dendrimers as biometric nanoprobe to detect vascular permeability. *J Mater Chem.* 2003; 13(7):1523–1525.
114. Siegal T, Horowitz A, Gabizon A. Doxorubicin encapsulated in sterically stabilized liposomes for the treatment of a brain tumor model: biodistribution and therapeutic efficacy. *J Neurosurg.* 1995; 83(6):1029–1037. [PubMed: 7490617]
115. Sharma US, Sharma A, Chau RI, Straubinger RM. Liposome-mediated therapy of intracranial brain tumors in a rat model. *Pharm Res.* 1997; 14(8):992–998. [PubMed: 9279878]
116. Hau P, Fabel K, Baumgart U, et al. Pegylated liposomal doxorubicin – efficacy in patients with recurrent high-grade glioma. *Cancer.* 2004; 100(6):1199–1207. [PubMed: 15022287]
117. Fabel K, Dietrich J, Hau P, et al. Long-term stabilization in patients with malignant glioma after treatment with liposomal doxorubicin. *Cancer.* 2001; 92(7):1936–1942. [PubMed: 11745268]
118. Moghimi SM, Szebeni J. Stealth liposomes and long circulating nanoparticles: critical issues in pharmacokinetics, opsonization and protein-binding properties. *Prog Lipid Res.* 2003; 42(6):463–478. [PubMed: 14559067]
119. Ishida T, Kiwada H. Accelerated blood clearance (ABC) phenomenon upon repeated injection of PEGylated liposomes. *Int J Pharm.* 2008; 354(1–2):56–62. [PubMed: 18083313]
120. Erickson BJ, Campeau NG, Schreiner SA, Buckner JC, O'Neill BP, O'Fallon JR. Triple-dose contrast/magnetization transfer suppressed imaging of 'non-enhancing' brain gliomas. *J Neurooncol.* 2002; 60(1):25–29. Clinical evidence that the short blood half-life of small-molecule MRI contrast agents such as Magnevist[®] is the primary reason that small CNS solid tumor foci often do not contrast enhance and are not visible on high-resolution scans. [PubMed: 12416542]
121. Pluen A, Boucher Y, Ramanujan S, et al. Role of tumor-host interactions in interstitial diffusion of macromolecules: cranial vs subcutaneous tumors. *Proc Natl Acad Sci USA.* 2001; 98(8):4628–4633. [PubMed: 11274375]
122. Koyama Y, Hama Y, Urano Y, Nguyen DM, Choyke PL, Kobayashi H. Spectral fluorescence molecular imaging of lung metastases targeting HER2/neu. *Clin Cancer Res.* 2007; 13(10):2936–2945. [PubMed: 17504994]
123. Adams GP, Schier R, McCall AM, et al. High affinity restricts the localization and tumor penetration of single-chain Fv antibody molecules. *Cancer Res.* 2001; 61(12):4750–4755. [PubMed: 11406547]

124. Lee CC, Gillies ER, Fox ME, et al. A single dose of doxorubicin-functionalized bow-tie dendrimer cures mice bearing C-26 colon carcinomas. *Proc Natl Acad Sci USA*. 2006; 103(45):16649. Utility of acid-labile covalent linkages for the conjugation of small molecule drugs to nanoparticles to facilitate timely drug release in the acidic environment of tumor cell endolysosomal compartments is demonstrated. [PubMed: 17075050]
125. Felgner PL, Gadek TR, Holm M, et al. Lipofection: a highly efficient, lipid-mediated DNA-transfection procedure. *Proc Natl Acad Sci USA*. 1987; 84(21):7413–7417. [PubMed: 2823261]
126. Herce HD, Garcia AE. Molecular dynamics simulations suggest a mechanism for translocation of the HIV-1 TAT peptide across lipid membranes. *Proc Natl Acad Sci USA*. 2007; 104(52):20805–20810. [PubMed: 18093956]
127. Herve F, Ghinea N, Scherrmann JM. CNS delivery via adsorptive transcytosis. *AAPS J*. 2008; 10(3):455. [PubMed: 18726697]
128. Sugahara KN, Teesalu T, Karmali PP, et al. Coadministration of a tumor-penetrating peptide enhances the efficacy of cancer drugs. *Science*. 2010; 328(5981):1031–1035. [PubMed: 20378772]
129. Harrison PM. The structure of apoferritin: molecular size, shape and symmetry from x-ray data. *J Mol Biol*. 1963; 6(5):404–422. [PubMed: 13953005]
130. Brightman MW. The distribution within the brain of ferritin injected into cerebrospinal fluid compartments I Ependymal distribution. *J Cell Biol*. 1965; 26(1):99–123. [PubMed: 5859025]
131. Armstrong JK, Wenby RB, Meiselman HJ, Fisher TC. The hydrodynamic radii of macromolecules and their effect on red blood cell aggregation. *Biophys J*. 2004; 87(6):4259–4270. [PubMed: 15361408]
132. Dellian M, Yuan F, Trubetskoy VS, Torchilin VP, Jain RK. Vascular permeability in a human tumour xenograft: molecular charge dependence. *Br J Cancer*. 2000; 82(9):1513–1518. [PubMed: 10789717]
133. Yuan F, Dellian M, Fukumura D, et al. Vascular permeability in a human tumor xenograft: molecular size dependence and cutoff size. *Cancer Res*. 1995; 55(17):3752. [PubMed: 7641188]
134. Yuan F, Leunig M, Huang SK, Berk DA, Papahadjopoulos D, Jain RK. Microvascular permeability and interstitial penetration of sterically stabilized (stealth) liposomes in a human tumor xenograft. *Cancer Res*. 1994; 54(13):3352–3356. [PubMed: 8012948]
135. Campbell RB, Fukumura D, Brown EB, et al. Cationic charge determines the distribution of liposomes between the vascular and extravascular compartments of tumors. *Cancer Res*. 2002; 62:6831–6836. [PubMed: 12460895]
136. Hobbs SK, Monsky WL, Yuan F, et al. Regulation of transport pathways in tumor vessels: role of tumor type and microenvironment. *Proc Natl Acad Sci USA*. 1998; 95:4607–4612. [PubMed: 9539785]
137. Thurston G, McLean JW, Rizen M, et al. Cationic liposomes target angiogenic endothelial cells in tumors and chronic inflammation in mice. *J Clin Inv*. 1998; 101(7):1401–1413.
138. MacKay JA, Deen DF, Szoka FC Jr. Distribution in brain of liposomes after convection enhanced delivery; modulation by particle charge, particle diameter, and presence of steric coating. *Brain Res*. 2005; 1035(2):139–153. [PubMed: 15722054]
139. Kamba T, Tam BYY, Hashizume H, et al. VEGF-dependent plasticity of fenestrated capillaries in the normal adult microvasculature. *Am J Physiol Heart Circ Physiol*. 2006; 290(2):H560–576. [PubMed: 16172168]
140. Luty GA, Hasegawa T, Baba T, Grebe R, Bhutto I, McLeod DS. Development of the human choriocapillaris. *Eye*. 2010:1–8.
141. Bearer EL, Orci L, Sors P. Endothelial fenestral diaphragms: a quick-freeze, deep-etch study. *J Cell Biol*. 1985; 100(2):418–428. [PubMed: 3968170]
142. Melamed S, Ben-Sira I, Ben-Shaul Y. Ultrastructure of fenestrations in endothelial choriocapillaries of the rabbit – a freeze-fracturing study. *Br J Ophthalmol*. 1980; 64(7):537–543. [PubMed: 7426569]
143. Matsumura Y, Maeda H. A new concept for macromolecular therapeutics in cancer chemotherapy: mechanism of tumoritropic accumulation of proteins and the antitumor agent SMANCS. *Cancer Res*. 1986; 46(12 I):6387–6392. [PubMed: 2946403]

144. Maeda H, Bharate GY, Daruwalla J. Polymeric drugs for efficient tumor-targeted drug delivery based on EPR-effect. *Eur J Pharm Biopharm.* 2009; 71(3):409. [PubMed: 19070661]
145. Kobayashi A, Oda T, Maeda H. Protein binding of macromolecular anticancer agent SMANCS: characterization of poly(styrene-co-maleic acid) derivatives as an albumin binding ligand. *J Bioact Compat Polym.* 1988; 3(4):319–333.
146. Oda T, Maeda H. Binding to and internalization by cultured cells of neocarzinostatin and enhancement of its actions by conjugation with lipophilic styrene–maleic acid copolymer. *Cancer Res.* 1987; 47(12):3206–3211. [PubMed: 2953411]
147. Oda T, Sato F, Maeda H. Facilitated internalization of neocarzinostatin and its lipophilic polymer conjugate, SMANCS, into cytosol in acidic pH. *J Natl Cancer Inst.* 1987; 79(6):1205–1211. [PubMed: 2961908]
148. Wu G, Barth RF, Yang W, et al. Site-specific conjugation of boron-containing dendrimers to anti-EGF receptor monoclonal antibody cetuximab (IMC-C225) and its evaluation as a potential delivery agent for neutron capture therapy. *Bioconj Chem.* 2003; 15(1):185–194.
149. Mross K, Niemann B, Massing U, et al. Pharmacokinetics of liposomal doxorubicin (TLC-D99; Myocet®) in patients with solid tumors: an open-label, single-dose study. *Cancer Chemother Pharmacol.* 2004; 54(6):514–524. [PubMed: 15322827]
150. Hersh EM, O'Day SJ, Ribas A, et al. A Phase II clinical trial of NAB-Paclitaxel in previously treated and chemotherapy-naive patients with metastatic melanoma. *Cancer.* 2010; 116(1):155–163. [PubMed: 19877111]
151. Kukowska-Latallo JF, Candido KA, Cao Z, et al. Nanoparticle targeting of anticancer drug improves therapeutic response in animal model of human epithelial cancer. *Cancer Res.* 2005; 65(12):5317–5324. [PubMed: 15958579]
152. Padilla De Jesus OL, Ihre HR, Gagne L, Frechet JMJ, Szoka FC. Polyester dendritic systems for drug delivery applications: *in vitro* and *in vivo* evaluation. *Bioconj Chem.* 2002; 13(3):453–461.
153. Tomalia DA, Reyna LA, Svenson S. Dendrimers as multipurpose nanodevices for oncology drug delivery and diagnostic imaging. *Biochem Soc Trans.* 2007; 35(Pt 1):61–67. [PubMed: 17233602]
154. Konda SD, Wang S, Brechbiel M, Weiner EC. Biodistribution of a 153Gd-folate dendrimer, generation = 4, in mice with folate-receptor positive and negative ovarian tumor xenografts. *Invest Radiol.* 2002; 37(4):199–204. [PubMed: 11923642]
155. Fukushima T, Takeshima H, Kataoka H. Antiglioma therapy with temozolomide and status of the DNA-repair gene MGMT. *Anticancer Res.* 2009; 29(11):4845–4854. [PubMed: 20032445]

Key Terms

Small-molecule chemotherapy drugs	Lipid-soluble and cationic lipid-soluble chemotherapy drugs in current clinical use that are less than 1–2 nm in diameter; these include the traditional chemotherapy drugs that target the cell cycle such as DNA alkylators and antimetabolites, as well as the newer drugs that target overexpressed cell membrane growth factor receptors and associated downstream cell-signaling pathways, which include tyrosine kinase and proteasome inhibitors
Interstitial fluid pressure	Sum of the hydrostatic and oncotic fluid pressures in the solid tumor interstitium, which are elevated in the solid tumor interstitium, being highest in the solid tumor center due to the absence of initial lymphatic capillaries in tumor center, and closer to normal in the tumor tissue periphery due to the presence of initial lymphatic capillaries in the tumor periphery
Vascular normalization	Low-to-moderate dose anti-VEGF pathway therapy aimed at regressing solid tumor blood capillaries as well as converting tumor blood capillaries to a more normal, less permeable phenotype; results

in a reduction in the elevated solid tumor interstitial fluid pressure, which is to promote the better, more homogenous distribution of adjuvantly administered small molecule chemotherapy drugs within the tumor interstitium

Theranostics

'All-in-one'-type particle to which therapeutic, imaging and/or targeting moieties are attached for the purposes of concurrent drug delivery, imaging of drug delivery, and targeting of specific over-expressed cell surface receptors or downstream signaling pathways (i.e. Gd-G5 doxorubicin dendrimer)

Endothelial glyocalyx layer

The innermost layer of the capillary wall; a polysaccharide-rich fibrous matrix of anionic proteoglycans and glycoproteins between 150 and 400 nm thick in the capillary walls of most normal tissue blood capillaries, and somewhat thinner in the capillary walls of solid tumor tissue blood capillaries; the individual fibers are arranged hexagonally and circumferentially spaced a maximum of 20 nm apart in the case of most normal tissue blood capillaries

Physiologic upper limit of pore size

Hydrodynamic diameter of the largest lipid-insoluble molecule that is restricted from passing through the pores in the capillary wall, and as such, constitutes the size of the molecule or macromolecule to which the pores in the capillary wall are impermeable, which in the case of VEGF-derived solid tumor blood capillaries is approximately 12 nm

Diaphragmed fenestrae

The 60 to 70 nm wide diaphragmed areas of the endothelial cells lining the capillary walls of VEGF-derived blood capillaries, which consist of a central membranous knob with several membranous septae radiating outward from the knob to the fenestral rim; the arc widths of openings devoid of membranous components have been measured to be up to 12 nm wide.

Executive Summary

- Focal CNS tumors can be effectively treated with locoregional therapies such as surgery and stereotactic radiotherapy; however, multiple metastatic solid tumor lesions in the CNS and infiltrative primary CNS solid tumors are difficult to effectively treat with these treatment modalities.
- Systemic chemotherapies in current clinical use also fail to effectively treat multiple metastatic solid tumor lesions in the CNS and infiltrative primary CNS solid tumors, as these chemotherapies are lipid-soluble and cationic lipid-soluble small molecule drugs, which are rapidly metabolized as well as filtered by the kidneys and do not accumulate to cytotoxic concentrations within the tumor cells of small solid tumor foci.
- Low-to-moderate dose anti-VEGF anti-angiogenic therapies reduce elevated interstitial fluid pressures in the solid tumor interstitium to promote the more homogenous distribution of small-molecule chemotherapy drugs within the tumor tissue interstitium through vascular normalization of the tumor blood capillary network; however, the additional clinical benefit of these therapies, in terms of increasing patient disease progression-free survival rates, is only a few additional months in most cases, which indicates that elevated tumor interstitial fluid pressure is not the primary reason for the ineffective accumulation of small molecule chemotherapy drugs in solid tumor cells.
- Small-molecule chemotherapy drugs do not remain at peak concentration in blood circulation for more than a few minutes and, therefore, the steep transcapillary concentration gradient favoring drug accumulation into the tumor interstitium is short lived and is the primary reason for the ineffective accumulation of small molecule chemotherapy drugs into solid tumor cells following bolus administration.
- The continuous systemic infusion of small molecule drugs improves the effectiveness of drug accumulation within the tumor interstitium; however, when these small drugs are administered over prolonged periods of time, drug fraction also distributes 'nonselectively' into interstitial spaces of otherwise normal healthy tissues via transcapillary passage through capillary walls, which results in significant treatment-associated short-term patient morbidity and long-term cognitive deficits.
- The blood capillaries of normal CNS tissues, other than those of the choroid plexus and the circumventricular organs, are nonfenestrated capillaries, which are impermeable to lipid-insoluble macromolecules; whereas the blood capillaries of all solid tumors larger than 1–2 mm³, including those of metastatic solid tumor lesions to the CNS as well as primary CNS tumors, are VEGF-derived fenestrated neo-angiogenic capillaries that are permeable to lipid-insoluble macromolecules.
- The aqueous pore openings of the diaphragmed fenestrae within the endothelial cell membranes of solid tumor blood capillaries permit the transcapillary extravasation of spherical macromolecules up to 12 nm in diameter in the case of solid tumors with volumes greater than 25–30 mm³, and that of macromolecules up to 10 nm in diameter in the case of solid tumors with volumes less than 25–30 mm³.
- Spherical particles 7 nm in diameter and larger are not cleared from blood circulation via renal filtration and, therefore, these particles maintain peak

concentrations over several hours in systemic blood circulation and do accumulate in the solid tumor interstitium for a sufficiently long time to accumulate to cytotoxic concentrations within individual solid tumor cells.

- The optimal particle-size range for spherical lipid-insoluble macromolecular systemic chemotherapies is between 7 and 10 nm as macromolecular therapies in this size range extravasate through the aqueous pores of the VEGF-derived fenestrated blood capillaries of solid tumors and accumulate over time to cytotoxic concentrations within individual solid tumor cells.
- Macromolecular systemic therapies with cationic exteriors are toxic to the endothelial glycocalyx and endothelial cell layers of all capillary walls and ‘nonselectively’ accumulate within normal tissues and organs.
- Lipid-insoluble macromolecular systemic therapies within the 7–10-nm size range, with a neutralized exterior, do not extravasate across the capillary walls of normal CNS tissue blood capillaries or across the capillary walls of most other normal non-CNS tissue blood capillaries, which are nonfenestrated blood capillaries; therefore, macromolecular systemic therapies in this 7–10-nm size range can accumulate ‘selectively’ to a great extent into solid tumor tissue.
- It is envisioned that optimally sized systemic therapies within the 7–10-nm size range will accumulate to therapeutic concentrations in solid tumor cells and effectively treat CNS and non-CNS solid cancers.

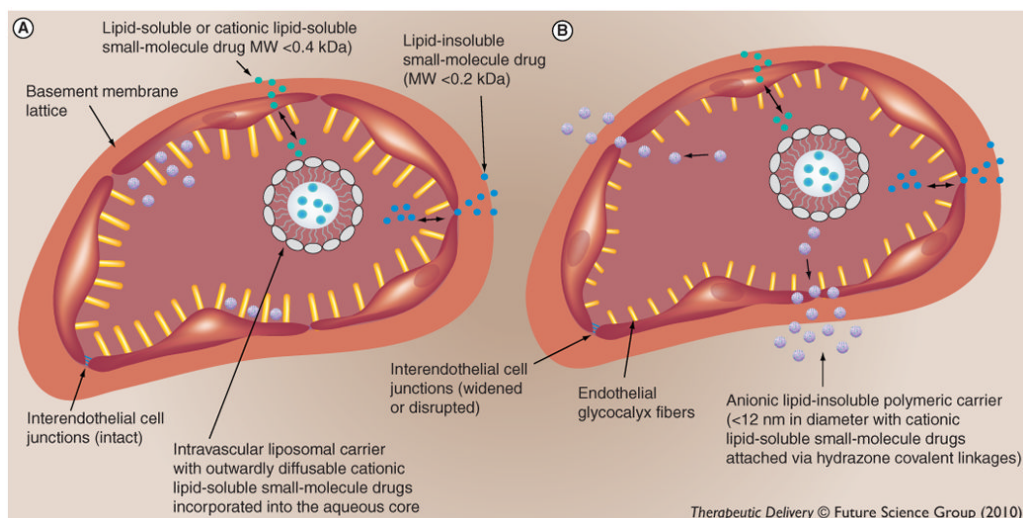


Figure 1. Capillary wall ultrastructures of normal brain and spinal cord parenchyma blood capillaries and VEGF-derived solid tumor blood capillaries and transcapillary routes for passage of small molecules and drugs and macromolecular systemic chemotherapies (A) Normal brain and spinal cord parenchyma blood capillary and (B) VEGF-derived solid tumor blood capillary. Capillary wall ultrastructures. Depicted are the three layers of the capillary wall. The yellow protrusions into the capillary lumen represent individual fibers of the polysaccharide-rich endothelial glycocalyx matrix with narrow interspacing. The bigger protrusions in (A) reflect the thicker glycocalyx of normal CNS tissue blood capillaries. The blue zona occludens interendothelial cell junctions between endothelial cells of normal brain and spinal cord parenchyma blood capillaries depict the intact functional interendothelial junctions of these blood capillaries, whereas the purple zona occludens interendothelial cell junctions of solid tumor tissue blood capillaries depict the disrupted dysfunctional interendothelial junctions of these blood capillaries. The small red domes represent the central membranous knobs of the diaphragmed fenestrae of the fenestrated endothelial cells of the VEGF-derived solid tumor blood capillaries. The pore openings of the diaphragmed fenestrae are wide enough to allow for the transcapillary passage of lipid-insoluble and cationic lipid-soluble molecules up to approximately 12 nm in diameter. The orange layer encircling the exterior of the endothelial cell lining layer depicts the collagenous lattice of the basement membrane layer. The basement membrane layers of both blood capillary types are depicted as being ultrastructurally similar, since the basement membranes of both blood capillary types are functionally intact. Transcapillary routes for passage of small molecules and drugs and macromolecular systemic chemotherapies. The small blue dots in the capillary lumens and the tissue interstitial spaces represent lipid-insoluble small molecules with molecular weights less than 0.2 kDa (e.g., electrolytes and nonelectrolytes), which can pass through the intact functional zona occludens interendothelial cell junctions of normal brain and spinal cord parenchyma blood capillaries and distribute into normal brain and spinal cord parenchyma interstitium during the time-period when the transcapillary concentration gradient is favoring forward diffusion from the capillary lumen into the tissue interstitium. The small green dots represent lipid-soluble molecule chemotherapy drugs with molecular weight less than 0.4 kDa (e.g., lomustine, 0.24 kDa), which can readily diffuse across the phospholipid bilayers of endothelial cell membranes and distribute nonselectively into normal healthy tissues, including normal brain and spinal cord parenchyma (shown), again, during the time-period when the transcapillary concentration gradient is favoring forward diffusion from the capillary lumen into the tissue interstitium. The small dots with a green exterior and blue interior represent charged cationic lipid-soluble small-molecule chemotherapy drugs of molecular weights greater than 0.4 kDa (e.g., doxorubicin, 0.54

kDa). Some are shown to be still encapsulated within the aqueous interior of a liposome, which is a large polymeric drug carrier for the purposes of sustained drug release, and remains within the capillary lumen, in the cases of both normal brain and spinal cord parenchyma and solid tumor blood capillaries. Those on the outside of the liposome represent the drug molecules that have diffused out of the liposome. Such free cationic lipid-soluble small drugs in the capillary lumen, although charged, cannot diffuse across the intact zona occludens interendothelial cell junctions of the capillary wall of normal brain and spinal cord parenchyma blood capillaries into normal brain and spinal cord parenchyma interstitium, which restrict the transcapillary passage of such charged drugs with molecular weights greater than 0.2 kDa. Such free cationic lipid-soluble small drugs in the capillary lumen, although lipid-soluble, also do not diffuse readily across the phospholipid bilayers of endothelial cell membranes, which restrict the transcapillary passage of such lipid-soluble small drugs with molecular weights greater than 0.4 kDa. The large structures containing multiple small dots represent anionic lipid-insoluble polymeric carriers less than 12 nm in diameter with cationic lipid-soluble small molecule drugs attached to the exterior via hydrazone covalent linkages (e.g., imageable dendrimer nanoparticles, with doxorubicin molecules covalently linked to surface groups via hydrolysable linkages, with diameters between 7 and 10 nm). Such lipid-insoluble polymeric drug carriers, with a neutralized exterior, upon systemic bolus administration, remain within the capillary lumens of normal brain and spinal cord parenchyma blood capillaries, but pass through the pore openings of the diaphragmed fenestrae of solid tumor blood capillaries and 'selectively' and 'homogenously' accumulate in the solid tumor tissue interstitium over time, delivering cytotoxic concentrations of chemotherapy drug into individual tumor cells.

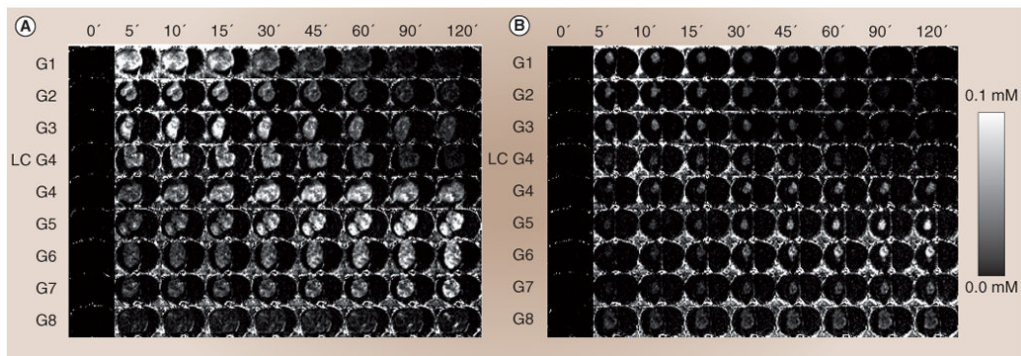


Figure 2. T₁-weighted dynamic contrast-enhanced MRI-based Gd-dendrimer distribution over time within larger and smaller orthotopic RG-2 rodent malignant gliomas

(A) Larger RG-2 gliomas; The volume, in mm³, for each large orthotopic RG-2 glioma: Gd-G1, 104; Gd-G2, 94; Gd-G3, 94; LC Gd-G4, 162; standard Gd-G4, 200; Gd-G5, 230; Gd-G6, 201; Gd-G7, 170; and Gd-G8, 289. (B) Smaller RG-2 gliomas; The volume, in mm³, for each small orthotopic RG-2 glioma: Gd-G1, 27; Gd-G2, 28; Gd-G3, 19; LC Gd-G4, 24; standard Gd-G4, 17; Gd-G5, 18; Gd-G6, 22; Gd-G7, 24; and Gd-G8, 107. Respective Gd-dendrimer generations administered intravenously over 1 min at a Gd dose of 0.09 mmol Gd/kg animal body weight. Scale from 0 mM [Gd] to 0.1 mM [Gd].

G: Generation; LC: Lowly conjugated.

Adapted with permission from [28].